



## Research article

## Robotic mirror therapy for stroke rehabilitation through virtual activities of daily living

Harris Nisar <sup>a</sup>, Srikanth Annamraju <sup>b,\*</sup>, Shankar A. Deka <sup>c</sup>, Anne Horowitz <sup>d</sup>, Dušan M. Stipanović <sup>b</sup><sup>a</sup> Health Care Engineering Systems Center, University of Illinois Urbana Champaign, 1206 W Clark St, Urbana 61801, IL, USA<sup>b</sup> Coordinated Science Laboratory, University of Illinois Urbana Champaign, 1308 W Main St, Urbana 61801, IL, USA<sup>c</sup> Division of Decision and Control Systems at KTH Royal Institute of Technology, Brinellvägen 8, 114 28 Stockholm, Sweden<sup>d</sup> Outpatient Rehabilitation, OSF Healthcare Saint Francis Medical Center, 6501 N Sheridan Rd, Peoria, IL, USA

## ARTICLE INFO

## ABSTRACT

## Keywords:

Robotic assistance  
Rehabilitation  
Mirror therapy  
Patient recovery  
Force feedback  
Nonlinear control

Mirror therapy is a standard technique of rehabilitation for recovering motor and vision abilities of stroke patients, especially in the case of asymmetric limb function. To enhance traditional mirror therapy, robotic mirror therapy (RMT) has been proposed over the past decade, allowing for assisted bimanual coordination of paretic (affected) and contralateral (healthy) limbs. However, state-of-the-art RMT platforms predominantly target mirrored motions of trajectories, largely limited to 2-D motions. In this paper, an RMT platform is proposed, which can facilitate the patient to practice virtual activities of daily living (ADL) and thus enhance their independence. Two similar (but mirrored) 3D virtual environments are created in which the patients operate robots with both their limbs to complete ADL (such as writing and eating) with the assistance of the therapist. The recovery level of the patient is continuously assessed by monitoring their ability to track assigned trajectories. The patient's robots are programmed to assist the patient in following these trajectories based on this recovery level. In this paper, the framework to dynamically monitor recovery level and accordingly provide assistance is developed along with the nonlinear controller design to ensure position tracking, force control, and stability. Proof-of-concept studies are conducted with both 3D trajectory tracking and ADL. The results demonstrate the potential use of the proposed system to enhance the recovery of the patients.

## 1. Introduction

Stroke is the third leading cause of death and disability combined. Each year, 12.2 million new strokes occur and one in four people over the age of 25 will have a stroke in their lifetime [1]. The high morbidity level of stroke leaves countless people disabled and in the need of specialized medical care, usually in the form of physical and occupational therapy [2]. Ischemic stroke (which accounts for 87% of strokes) leads to damage in a particular part of the brain due to lack of blood flow to that region [3]. Following an ischemic stroke within the motor cortex, one or more body parts contralateral to the infarct are impaired or paretic, which is known as hemiparesis in the case of partial paralysis and hemiplegia in the case of complete paralysis. It has been estimated that 80% of stroke survivors must live with motor impairments and 50% of hemiplegic patients never regain motor function [4,5]. Motor impairments lead to the inability to perform activities of daily living (ADL) which decreases independence in stroke survivors [4]. There is a strong

correlation between ADL performance and a survivor's quality of life [6].

A commonly utilized therapy technique for patients suffering from limb hemiparesis to recover motor function is mirror therapy. In this technique, the patient places their paretic limb behind a mirror and moves their healthy limb in front of the mirror. This creates the illusion that the paretic limb is fully controllable by the patient [7]. The illusion of coordinated movements between both limbs has been shown to be enough to regain motor function [8,9]. An extension of traditional mirror therapy is asking the patient to perform coordinated bilateral movements with both limbs, which is known to cause interactions between the patient's damaged and undamaged brain regions [10,11]. This interaction induces neuroplasticity, which is the brain's ability to reorganize by developing new neural connections due to sensory input, experience, and learning [12].

To expedite the rehabilitation process and facilitate higher frequency of therapy sessions, robotic mirror therapy (RMT) techniques have been

\* Corresponding author.

E-mail address: [annamra2@illinois.edu](mailto:annamra2@illinois.edu) (S. Annamraju).

proposed in the literature where the paretic limb moves (as opposed to the mirror illusion). For instance, in [13], the patient is asked to handle two similar robots. While the patient makes motions with their contralateral arm, the other robot is programmed to perform a mirrored motion, thus enabling the mirrored motion of the paretic arm. This approach is limited to 2D trajectories without any specific context. In a more recent work [14], an attempt is made to use reinforcement learning which accounts for trajectories and patient's emotions to enhance safety. Another learning-based approach is presented in [15] to ensure that the impaired limb always gets safe trajectories to follow. An impedance model is considered here for the human-robot interaction so that the patient's trajectories are always smooth.

Although researchers are currently developing custom specific devices for RMT [16,17], very few of them cater to daily life task-oriented training. It has been found that task-oriented training, which is meant to enhance skills by practicing meaningful functional activities, is associated with beneficial neuroplastic changes. This change is found to be significantly greater than those seen in patients undergoing conventional exercise programs [18,19]. Even in those works which deal with ADL, the patient's robot is automated to make mirrored motions. This brings out a need for developing RMT framework with ADL incorporated which allows the patient to not just make automated motions but allow them to independently control their robots. To simulate many functional activities reasonably in a robotic setting, 3D tracking is required which is not explored in current RMT systems.

In this work, we have developed an RMT framework for the rehabilitation of patients with upper limb hemiparesis. In our proposed framework, the patient operates two physical robots with their upper limbs in two mirrored virtual environments. These virtual environments are visualized by the participants on a monitor. Throughout the session, the therapist (red fork in Fig. 1) can lead the patient's contralateral limb (blue fork in Fig. 1). The mirror of the patient's contralateral limb leads the patient's paretic limb (green fork in Fig. 1). A recovery level that is inversely proportional to the position error between each of the patient's limbs and its leader is calculated. An assistive force is provided to the patient's limbs through their corresponding robots and this force is scaled by the limb's recovery level to passively assist the limb in following its leader. In addition to the assistive forces, all three limbs experience complete force feedback from the virtual environment which allows for the creation of realistic simulations of ADL. The proposed framework aims to accomplish the following: (i) the recovery of the patient's motor ability to accurately follow the therapist (which involves shoulder to wrist joint motions), (ii) the recovery of the patient's vision and cognitive abilities due to the coordinated motions between both limbs along with visualizing the 3D tracking task through a 2D visualization, (iii) the induction of neuroplasticity in the patient due to the coordinated bilateral movements and the task-oriented nature of the therapy, and (iv) the maintenance of the patient's motivation levels since the therapy is now task-oriented and "gamified" with feedback scores which is crucial when undergoing intensive rehabilitation [20, 21]. This work is summarized in Fig. 1, which shows a comparison

between traditional approach, state-of-the-art RMT, and the proposed RMT.

Using this framework, two therapy tasks are implemented. In the first task, the patient completes coordinated movements in the form of 3D mirrored trajectory tracking. In the second task, the patient is asked to complete mirrored ADL. Specifically, they are tasked with transferring food between a set of plates. The second task builds on the first one in difficulty since the patient must understand the goals of the ADL along with completing the task. While the therapist can lead the therapy session in either task, their involvement is optional to allow for independent completion of rehabilitation.

To ensure the safety and reliability of the framework, the mathematical models of the robots' dynamical systems are considered. Nonlinear controllers are designed to accomplish the implementation of the rehabilitation tasks through position and force tracking. The system's global stability is proven using passivity analysis to ensure safe operation for the patient and therapist. Furthermore, the controllers do not require gain tuning which allows them to be used as is by therapists for a variety of patients. However, the controllers can be modified for each limb in an understandable way by the therapist through a few parameters that can scale the assistance level.

The rest of the paper is organized as follows: first the framework and its features are outlined in more detail. Second, the tasks implemented with this framework are discussed. Third, the controllers needed to implement these features and tasks are developed and analysed. Fourth, the framework is implemented in an experimental testbed to validate the features with healthy subjects.

## 2. Proposed framework

A framework which has several features to allow for robotic mirror therapy is presented here. These features will be used to create rehabilitation tasks that will be described in later sections.

### 2.1. Robotic rehabilitation setting

The therapist is provided with one robot, and the patient is provided with two robots – one for each limb. The robots are dexterous enough to provide manipulability for all the affected joints. While the therapist manipulates their robot, the end-effector is visualized on a screen. The patient attempts to track the therapist with their contralateral limb and to track the mirror of the contralateral limb with their paretic limb. The end-effectors of these robots are also visualized.

#### Recovery Level.

The position tracking errors for both limbs are constantly recorded to monitor the instantaneous recovery level,  $r(t) \in [0, 1]$ , of the patient. To calculate the contralateral limb's recovery,  $r_c(t) \in [0, 1]$ , first the error between the therapist and patient's contralateral limb,  $\hat{e}_c(t)$ , is calculated as

$$\hat{e}_c(t) = f(x_{th}(t), x_c(t)) \quad (1)$$

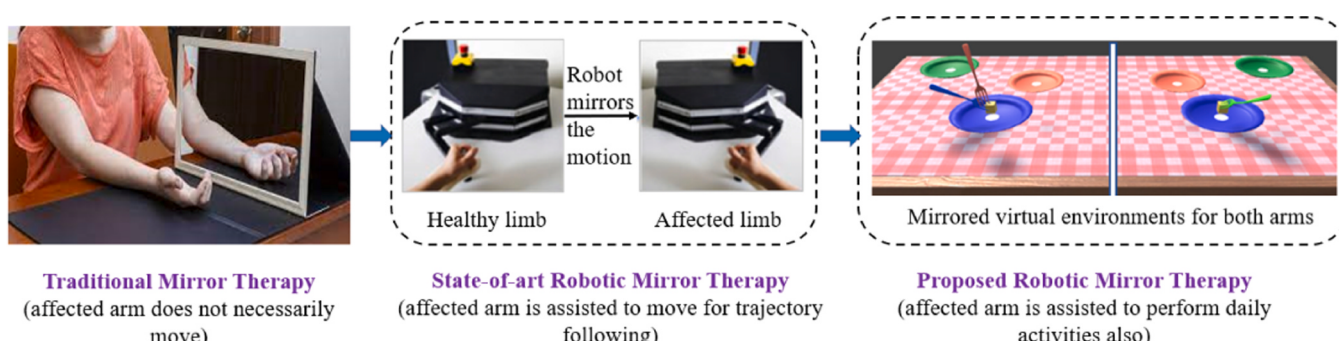


**Fig. 1.** Traditional and state-of-the-art RMT in comparison with proposed RMT with ADL.

where  $f : (R^3, R^3) \rightarrow R$  is the error function,  $x_{th}(t) \in R^3$  is the 3D Cartesian coordinates of the end-effector controlled by the therapist, and  $x_c(t) \in R^3$  is the position of the end-effector controlled by the contralateral limb of the patient. In this implementation, Euclidean distance is used as the error function for its ease of implementation and analysis and to keep the presentation easy to follow. However, the framework allows for more complex error functions. Then,  $r_c(t)$  is

$$r_c(t) = 1 - \frac{\widehat{e}_c(t)}{e_0} \quad (2)$$

where  $e_0$  is the maximum possible error, resulting in a  $r_c(t)$  that is between 0 and 1. Similarly, to calculate the paretic limb's recovery,  $r_p(t)$ , the error between the mirrored contralateral and paretic limbs,  $\hat{e}_p(t)$ , is calculated as

$$\hat{e}_p(t) = f(\tilde{x}_c(t), x_p(t)) \quad (3)$$

where  $\tilde{x}_c(t) \in R^3$  is the mirrored position of the end-effector controlled by the contralateral limb of the patient and  $x_p(t) \in R^3$  is the position of the end-effector controlled by the paretic limb of the patient. Then,  $r_p(t)$  is computed as

$$r_p(t) = 1 - \frac{\widehat{e}_p(t)}{e_0} \quad (4)$$

A weighted average between both  $r_c(t)$  and  $r_p(t)$  is computed as the overall recovery level of the patient as follows:

$$r(t) = \alpha \cdot r_c(t) + \beta \cdot r_p(t) \quad (5)$$

where  $\alpha$  and  $\beta$  are scalars determined by the therapist per patient.

## 2.2. Adaptive assistance level

An adaptive assistance is provided to both the patient's limbs through the robots to assist them in tracking their corresponding leader. For example, the contralateral limb receives assistance so that it can track the therapist. The direction of this assistance is determined by the normalized vector formed between the therapist and the contralateral limb. The magnitude is determined to be  $\gamma(1 - r_c(t))$ , where  $\gamma$  is a constant scaling factor, in Newtons, which is decided by the therapist for each specific patient. A similar computation is done for the paretic limb with a different scaling factor ( $\sigma$ ). For instance, a patient who is just beginning rehabilitation is expected to need more assistance than one who has already gone through multiple sessions, especially on the robotic platform. Another consideration in choosing the scaling factor is the severity of stroke impact on the patient. A similar procedure is followed to determine the assistance level supplied to the patient's paretic limb.

### *2.3. Environmental force feedback*

The therapist and patient can navigate virtual environments with their robots. While interacting with objects in virtual environments, the robots are programmed to supply feedback forces from the objects in the environments. This enables both the therapist and patient to perceive the environment accurately. Fig. 2 shows the signal flow of the framework.

### 3. Rehabilitation tasks

With the framework presented in Section 2, the tasks of trajectory tracking and practicing simulated ADL are described below.

### 3.1. Task 1: Trajectory tracking

In this task, the therapist can freely draw symbols with their robot. The patient must track the therapist as described in 2.1. Features mentioned in 2.2 and 2.3 are sufficient to assist the patient's limbs in tracking. In addition, predefined trajectories can also be visualized on the screen as a reference for tracking. In either case, the proposed framework gives the advantage over traditional mirror therapy since it does not obscure the patient's vision while the therapist is assisting.

### 3.2. Task 2: ADL practice

To allow the patient to practice ADL, a dining virtual environment is created. A second, identical environment is also created that is the mirror of the first. The therapist and the contralateral limb operate in the first environment and the paretic limb operates in the mirrored environment. The therapist leads the contralateral limb to pick up virtual food from one plate and place it on another. The paretic limb must complete the same task but mirrored in the mirrored environment. All the features detailed in 2 are simultaneously utilized in this task.

#### 4. Controller design

#### 4.1. Dynamical model of the system

To ensure position tracking for both tasks, and the force tracking in task 2, nonlinear controllers are developed. The three physical robots are first modeled using Lagrangian dynamics, which take the following form:

$$M_{th}(q_{th})\ddot{q}_{th}(t) + C_{th}(q_{th}, \dot{q}_{th})\dot{q}_{th} + G_{th}(q_{th}) = \tau_{th} - \tau_{th,a} \quad (6)$$

$$M_c(q_c)\ddot{q}_c(t) + C_c(q_c, \dot{q}_c)\dot{q}_c + G_c(q_c) = \tau_c - \tau_{c,a} \quad (7)$$

$$M_n(q_n)\ddot{q}_-(t) + C_n(q_n, \dot{q}_-) \dot{q}_- + G_n(q_n) \equiv \tau_n - \tau_{n,a} \quad (8)$$

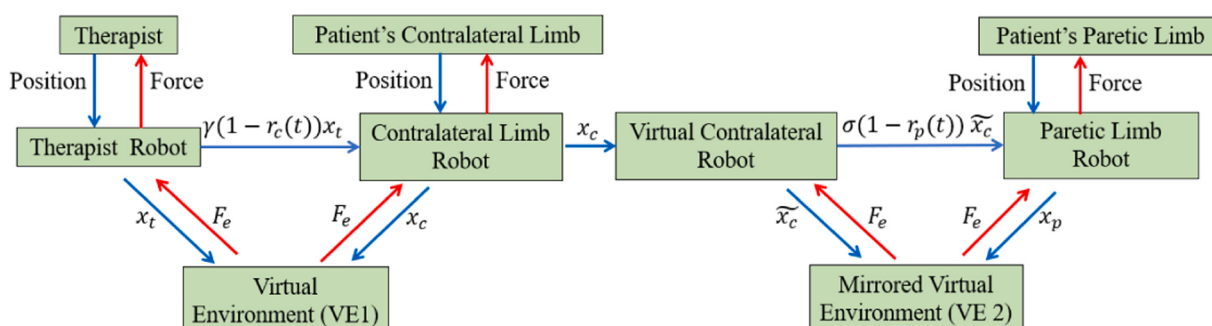


**Fig. 2.** Signal flow of the proposed framework.

$q \in \mathbb{R}^{nx1}$  represents the joint variables of the corresponding robot,  $\tau_{th} \in \mathbb{R}^{nx1}$ ,  $\tau_c \in \mathbb{R}^{nx1}$ , and  $\tau_p \in \mathbb{R}^{nx1}$  represent the external torque applied by the therapist, contralateral limb, and paretic limb respectively,  $\tau_{th,a} \in \mathbb{R}^{nx1}$ ,  $\tau_{c,a} \in \mathbb{R}^{nx1}$ , and  $\tau_{p,a} \in \mathbb{R}^{nx1}$  represent the joint torques of the therapist, contralateral, and paretic limb robots, respectively. The positions and torques are all time dependent, but the expression is omitted to maintain brevity.

#### 4.2. Control objectives

For the therapist's robot, the only control objective would be to render force feedback when there is interaction with the virtual environment, which happens only in task 2. Thus, in task 1, the therapist's robot practically requires no controller design. For each of the patient's robot, regardless of the task, the controller design should ensure accurate position tracking, and specifically for task 2, an additional force control objective is needed to obtain environmental force feedback. The controllers are now developed using passivity.

#### 4.3. Theory of passivity

The interconnection of multiple passive systems being again passive (which is not necessarily true with stability) under the scattering matrix condition [22], makes it an appropriate tool for analysing systems such as leader-follower robots. The output strictly passive nature of each sub-system (with input  $u$  and output) is proven by choosing a positive semi-definite function  $S$  such that  $\dot{S} \leq y^T u - \delta_y y^2$ . Global asymptotic stability is then inferred for the passive system by checking the storage function for radial unboundedness and the system for zero-state observability, i.e., the zero vector being the only set of states satisfying the input and output simultaneously being zero [23].

#### 4.4. Position controller for patient's robots

The position controller for the contralateral limb is proposed as

$$\begin{aligned} \tau_{c,a,p}(t) = & u + G_c + C_c \dot{q}_{th}(t) + M_c \ddot{q}_{th}(t) + \tau_c(t) - k_p(q_c(t) - q_{th}(t)) \\ & - k_v(\dot{q}_c(t) - \dot{q}_{th}(t)) \end{aligned} \quad (9)$$

where  $k_p, k_v \in \mathbb{R}$  are the controller gains. A similar position controller would be used for the paretic limb's robot to track the mirror of the contralateral limb, where the following transformation is used to compute  $\tilde{x}_c(t)$

$$\tilde{x}_c(t) = \tilde{M} \cdot x_c(t) \quad (10)$$

where  $\tilde{M} \in \mathbb{R}^{3 \times 3}$  is the mirroring diagonal matrix with 1 along the diagonal elements corresponding to the mirror plane's axes and  $-1$  at the element corresponding to the axis which is perpendicular to the mirror plane. To obtain the mirrored positions in joint space ( $\tilde{q}_c(t)$ ), the inverse kinematics of the robot is used to transform the Cartesian coordinates. When the controller in (9) is incorporated into the contralateral limb's robot dynamics (7), the modified dynamics of the contralateral limb's robot are given by

$$M_c(\ddot{q}_c(t) - \ddot{q}_{th}(t)) + (C_c + k_v I)(\dot{q}_c(t) - \dot{q}_{th}(t)) + k_p(q_c(t) - q_{th}(t)) = u \quad (11)$$

where  $I_{n \times n}$  refers to the identity matrix. Let  $e_c$  denote the position tracking error term of the virtual robot, i.e.,  $q_c(t) - q_{th}(t)$ . The modified dynamics (11) can be rewritten as

$$M_c \ddot{e}_c(t) + (C_c + k_v I) \dot{e}_c(t) + k_p e_c(t) = u. \quad (12)$$

The system shown in (12) now represents the modified dynamics of the system, and hence, passivity analysis is performed on it. Passivity is proven by choosing the positive semidefinite and radially unbounded storage function as

$$S = \frac{1}{2} \dot{e}_c^T M_c \dot{e}_c + \frac{1}{2} \dot{e}_c^T k_p \dot{e}_c. \quad (13)$$

The time derivative of this storage function is given by

$$\dot{S} = \dot{e}_c^T M_c \ddot{e}_c + \frac{1}{2} \dot{e}_c^T \dot{M}_c \dot{e}_c + e_c^T k_p \dot{e}_c. \quad (14)$$

Substituting the value of  $M_c \ddot{e}_c$  from the modified dynamics (12) into (14), we have

$$\dot{S} = \dot{e}_c^T u + \frac{1}{2} \dot{e}_c^T (\dot{M}_c - 2C_c) \dot{e}_c + k_p(e_c^T \dot{e}_c - \dot{e}_c^T e_c) - k_v \dot{e}_c^T \dot{e}_c. \quad (15)$$

Since  $\dot{M}_c - 2C_c$  is skew-symmetric as per the well-known Lagrangian property [24],  $\dot{e}_c^T (\dot{M}_c - 2C_c) \dot{e}_c$  is always zero. Similarly, for any column vector  $e_c$ ,  $e_c^T \dot{e}_c - \dot{e}_c^T e_c$  becomes zero. Thus, (15) is simplified to

$$\dot{S} = \dot{e}_c^T u - k_v \|\dot{e}_c\|^2 \quad (16)$$

where  $\|\cdot\|$  represents the 2-norm of the argument.

The result in Eq. (16) reveals that the system under consideration is output strictly passive from input  $u$  to output  $\dot{e}_c$  (by the definition presented in Section 4.3). To further validate the zero-state observability of the system, the input and output values are set to zero in the modified dynamics shown in (12). This leads to  $q_c = 0$ , indicating the accurate position tracking of the contralateral limb robot. A typical application of LaSalle's invariance theorem is performed here to deduce the zero-state observability [23,25]. Making the choice of error being the state, the system's zero-state observability also follows.

Since all the three requirements - output strictly passivity, zero-state observability, and radially unbounded storage function are met, the system can be certified as globally asymptotically stable. Since (16) assures passivity of the system irrespective of the feedback gains in the controller, the system is stable for any positive value of gain. This reduces the process of gain tuning, which is a tedious process in nonlinear systems.

#### 4.5. Force controller for patient's robots

The proposed force controller for the contralateral limb's robot which ensures accurate perception of the environment is

$$\begin{aligned} \tau_{c,a,f} = & -u - G_c - C_c \dot{q}_{th} - M_c \ddot{q}_{th} + \tau_c + k \dot{e}_c + \frac{1}{2} (\tau_c - \tau_e)^T (\tau_c - \tau_e) \dot{e}_c \\ & + \left( \int_0^t (\tau_c - \tau_e)^T (\tau_c - \tau_e) dt \right) \dot{e}_c + (\text{sgn}(\dot{e}_c + \varepsilon) (\tau_c - \tau_e)^T (\tau_c - \tau_e) \dot{e}_c) \end{aligned} \quad (17)$$

where  $\tau_e \in \mathbb{R}^{nx1}$  is the environmental torque,  $\text{sgn}(\cdot)$  represents signum function,  $k \in \mathbb{R}$  is the controller gain,  $\varepsilon \in \mathbb{R}$  is a small positive quantity.

Incorporating the proposed controller (17) into the dynamics (7) gives the modified dynamics as

$$\begin{aligned} M_c + & \left( \int_0^t (\tau_c - \tau_e)^T (\tau_c - \tau_e) dt \right) \dot{e}_c + \left( C_c + \frac{1}{2} (\tau_c - \tau_e)^T (\tau_c - \tau_e) + k \right) \dot{e}_c \\ & + (\text{sgn}(\dot{e}_c + \varepsilon) (\tau_c - \tau_e)^T (\tau_c - \tau_e) \dot{e}_c) = u. \end{aligned} \quad (18)$$

To prove the system as output-strictly passive, the radially unbounded storage function chosen as

$$S = \frac{1}{2} \dot{e}_c^T M_c \dot{e}_c + \frac{1}{2} \dot{e}_c^T \left( \int_0^t (\tau_c - \tau_e)^T (\tau_c - \tau_e) dt \right) \dot{e}_c. \quad (19)$$

Upon taking the time derivative and simplifying, we obtain

$$\dot{S} = \dot{e}_c^T u - k \|\dot{e}_c\|^2 - \dot{e}_c^T (\text{sgn}(\dot{e}_c + \varepsilon) (\tau_c - \tau_e)^T (\tau_c - \tau_e) \dot{e}_c). \quad (20)$$

The last term of (20) is now analyzed to validate the 'output strictly passivity' of the system. It is evident that  $(\tau_c - \tau_e)^T (\tau_c - \tau_e) \geq 0$ . Furthermore, whether  $\dot{e}_c$  is positive or negative, the term  $\dot{e}_c^T (\text{sgn}(\dot{e}_c) + \varepsilon) (\tau_c - \tau_e)^T (\tau_c - \tau_e) \dot{e}_c$  is



**Fig. 3.** Experimental setup.

$\varepsilon) > 0$ . The minimal value the last term of (20) can take is 0 when  $\dot{e}_c = 0$ . In either case,  $(\tau_c - \tau_e)^T(\tau_c - \tau_e) \geq 0$ . Thus, (20) simplifies to

$$\dot{S} = \dot{e}_c^T u - k \|\dot{e}_c\|^2. \quad (21)$$

Since the system is found to be passive from  $u$  to  $\dot{e}_c$  (mentioned in Section 4.3), zero input and output in the modified dynamics leads to

$$(\text{sgn}(\dot{e}_c) + \varepsilon)(\tau_c - \tau_e)^T(\tau_c - \tau_e). \quad (22)$$

Since  $\varepsilon > 0$  and  $\text{sgn}(\dot{e}_c) = 0$  for  $\dot{e}_c = 0$ , we can conclude that  $\tau_c - \tau_e = 0$ , which indicates the accurate force tracking of the contralateral limb robot.

Further, choosing  $\dot{e}_c$  itself as the state of the system, the system is also zero-state observable. Owing to radially unbounded  $S$ , the system is globally asymptotically stable, which is again independent of the controller gain,  $k$ .

The controller design in this sub-section can render force feedback from the environment to the contralateral limb. The contralateral limb will actually be provided with a hybrid controller of (9) and (17) as illustrated in [26]. This hybrid algorithm performs like an impedance model and ensures that the limb can accurately track the therapist's robot, receive assistance from its robot, and experience the feedback forces from the environment simultaneously, all while maintaining stability.

Controllers with exactly similar structures along with their corresponding storage functions are proposed for realizing the force feedback for the therapist and the paretic limb. The proof follows in the same manner as detailed above. The only difference for the therapist's force controller would be that since the therapist does not need to track any other robot, the velocity error term is replaced by zero.

## 5. Experiments and results

### 5.1. Experimental setup

The three physical robots chosen for experiments are the 3D Systems® Touch haptic devices. These were chosen due to their 6 degrees of freedom dexterity and their capability to render joint motions at all the arm motor joints – shoulder, elbow, and wrist. These haptic devices operate within a limited workspace and the velocities and torques of the device at each joint are saturated, thus minimizing any risk to the operator. The therapist is given one robot and the patient is given two (one for each limb). The controllers proposed in Section 4 are implemented with all the three robots physically connected to each other in a daisy chain through a wired ethernet communication channel. Since all the 3 robots are in the same console, the delays in serial communication are negligible. Two screens are placed in the console where both the therapist and the patient can conveniently visualize their motions in the tasks discussed above. Unity 3D is used to interface with robots and to implement the features of the framework along with the tasks. The

experimental testbed is shown in Fig. 3. In these experiments, healthy subjects pretended to be the therapist and patient.

### 5.2. Computation of recovery level

To ensure that  $r(t) \in [0, 1]$ , the maximum possible error the corresponding patient's arm can make (denoted by  $e_0$ ) is determined. The maximum distance on the robot's outer workspace for any 2-point combination is determined, where the workspace is defined by a cube of with dimensions 431 W x 384 H x 165 D mm. Given the fact that the patient cannot make an error larger than this while following another robot with the same workspace, this maximum distance is considered as  $e_0$ . Another approach of computing  $e_0$  which is independent of the robot used track the maximum error made during a session. Using either of these approaches would result in both the recovery levels being in the range of 0–1. However, in the latter approach, the value of  $e_0$  for both the recovery levels in (2) and (4) would not be the same. The former approach is used here. The implementation architecture is summarized in Fig. 4.

### 5.3. Task 1: Trajectory tracking

As explained in Section 2.1, the patient is first taken through a preliminary task, before beginning the ADL. The objective of this task is to get the patient familiar with RMT and to have them perform some simpler tasks before delving into ADL. This phase could either engage the patient in following the custom specific trajectories of the therapist (in 3D) or drawing some specific pre-defined symbols without the active involvement of the therapist. In the latter case, a certain predefined trajectory is displayed on the screen, and the patient is asked to trace it (as shown in Fig. 5). In Fig. 5, a circle of radius 10 cm is taken as the reference. Active involvement of the therapist (with their robot) can ensure that the patient gets therapy on all the necessary joint motions, which may not be captured through pre-defined symbols and can also keep the patient engaged. The choice of the therapist being in the loop is typically made by the therapist based on the motor abilities of the patient assessed through standard techniques such as Fugl-Meyer [27].

Experiments are conducted where the subject simulating the patient is asked to follow the 3D trajectories of the subject simulating the therapist with both the limbs. The therapist was instructed to make oscillatory trajectories and operated at approximately 0.075 Hz. During the first cycle of the experiment, the subject is told to offer high resistance while following the contralateral limb with their paretic limb. During the second and third cycles, they offer medium and low resistances respectively. This is meant to simulate a growing recovery factor as the tracking improves. The assistive forces mentioned in Section 2.3 are supplied and the position tracking results obtained are presented in Fig. 6.

It can be seen from Fig. 6 that the contralateral arm always tracks the therapist in all three coordinates, while the paretic arm tries to track the

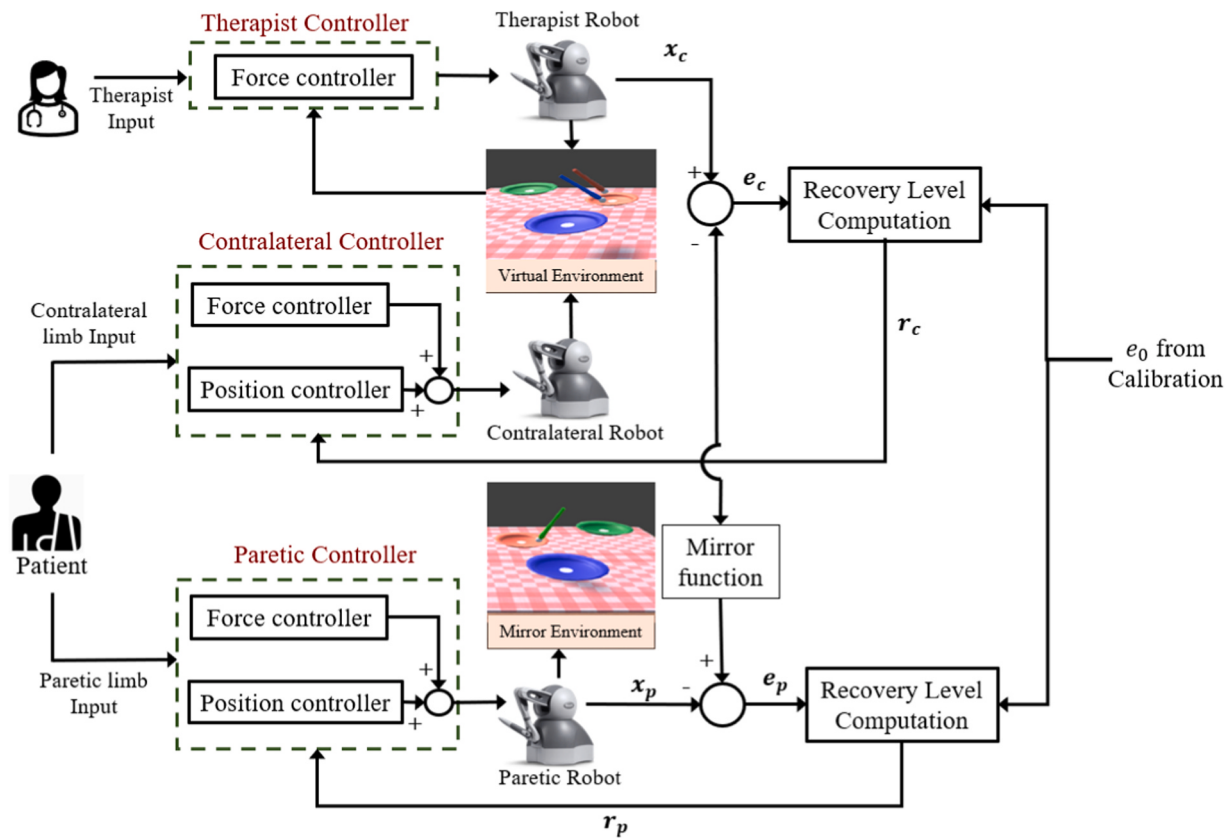


Fig. 4. Experimental implementation.

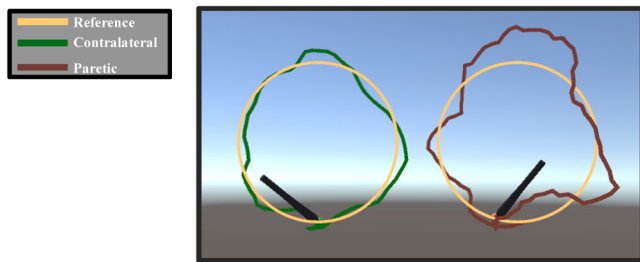


Fig. 5. Patient following pre-defined symbols.

mirrored position of the healthy arm. The mirroring in this case is taken along the  $x$ -axis, and thus the positions in  $x$ -coordinate alone are mirrored. There is always a delay in the contralateral arm following the therapist (approximately 0.9 s), and the paretic arm following the contralateral limb (approximately 0.7 s), which is realistic because it takes some time to interpret the visual cues of the leader. As the patient improves, the delay eventually approaches 0 s. The corresponding tracking errors that are computed as per (1) and (3) are shown in Fig. 7.

It is to be noted that the errors in  $x$  and  $y$ -coordinates converge to zero over time, but the error in  $z$ -coordinate sustains to a reasonable degree. This shows that along  $z$ -axis, which is the depth in the designed experiment, the subject's perception is poor.

The recovery level of both the contralateral and paretic limbs and the assistance needed by each of them to perform this task are also reported in Fig. 8. Both these parameters are quantitative metrics to evaluate the patient's growth and are unitless.

At the start, when the subject is told to resist, the recovery level is the lowest (0.67 and 0.55 for the contralateral and paretic limb, respectively) and the assistance level is the highest. As the subject eases their

level of resistance, the recovery level in both limbs improves to be over 0.9. As the subject reduces resistance, the assistance needed for the corresponding arm also reduces proportionately and it can be seen from Fig. 8 that by the end of the session, the patient is able to follow the trajectories with an assistance which is about  $1/10^{th}$  of the initial assistance. The results here are meant to demonstrate that the recovery level behaves as expected and not to indicate that the system can recover a patient in the given time frame. Several such sessions will be required for improving patient performance and will be explored in future works.

#### 5.4. Task 2: Pick-and-place

##### 5.4.1. Pick-and-place tracking

A sample task of 'pick-and-place', which is ubiquitous in daily life, is chosen as the proof-of-concept ADL. Fig. 9 shows the visualization of the virtual environment which involves two sub-environments that are mirror images of each other.

The left half of the environment is where patient's contralateral limb (blue fork in Fig. 9) and therapist (red fork in Fig. 9) operate, and the right half is where the paretic limb (green fork) operates. A virtual piece of food (yellow cube in Fig. 9) is placed at the center of each blue plate. The task of the subject simulating the patient is to move the food between the centers of the red, green, and blue plates (in that order) for 3 cycles. The therapist could also guide the patient by leading their contralateral limb through their robot. However, since the example of therapist-in-the-loop is already depicted in task 1, the case study of patients performing the task independently is shown here. The accuracy in placing the food at the center of the plates and the coordination levels in exactly mirroring both arms are measured. The position of the food in each sub-environment (contralateral side and paretic side) is provided in Fig. 10. The positions of the plates are also marked. Note that the mirroring effect is undone to allow for easier comparison.

As expected, the food is moved between the plates as described in the

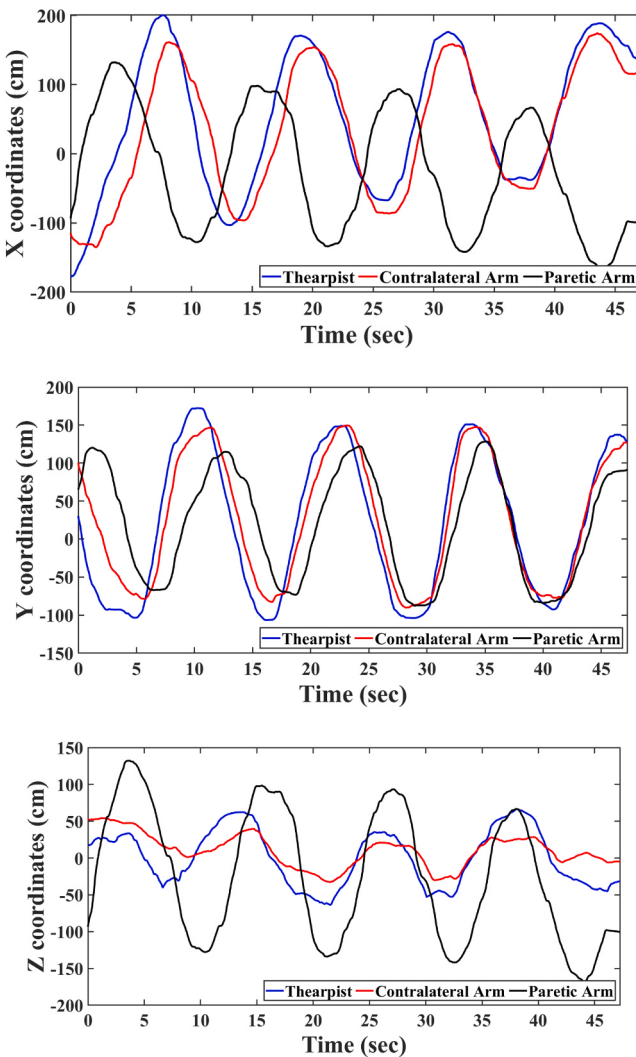


**Fig. 6.** Patient's 3D trajectory tracking.

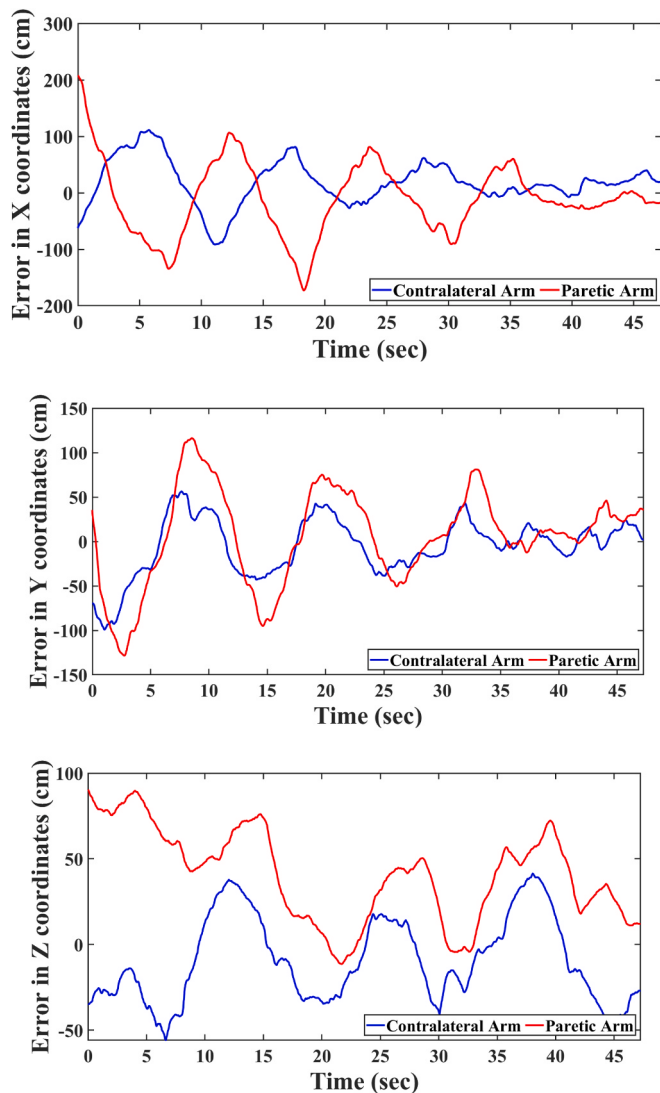


**Fig. 7.** Trajectory tracking errors.

instructions. Additionally, while the  $x$  and  $z$ -coordinates of the food are realistically close enough to the plate positions, the  $y$ -coordinates in each turn and at each plate exactly match. This is only because, the vertical (up-down) motion is designated as the  $y$ -coordinate, and even if the subject does not exactly reach the surface of the plate along  $y$ -axis, the food drops by gravity onto the plate and the position is recorded as exactly equal to that of the plate.

#### 5.4.2. Pick-and-place environmental force feedback

To verify the complete force feedback exerted by the virtual environment, the same 3-plate virtual environment described above is utilized. To simulate an ADL scenario, stiffness, damping, and inertia values can be independently assigned to all the objects in the virtual environment. This makes each object behave as a mass-spring-damper system, rendering a specific feedback force to the operator through the haptic device when they interact with it. These mechanical properties were chosen empirically based on what gave realistic force feedback. In the case of the pick-and-place activity, the table and plates are simulated as masses (20 kg and 30 g respectively). The subject is asked

to push each of the three plates once in the same order (red→green→blue). The corresponding positions recorded from the robots and the forces experienced by the user are reported in Fig. 11.

When the operators hit and are trying to push the plates (approximately  $t = 2.55\text{--}5.34, 8.36\text{--}10.53$  and  $13.67\text{--}16.10$ ), the positions of the robots remain almost constant indicating the plates' ability to resist the motion. This naturally induces the patient to exert at least a little additional force than they are used to, thus facilitating their recovery of muscle memory. Furthermore, for each of the three operating arms, full force-feedback from the virtual environment is transferred.

To make the data recorded during the therapy session more accessible to the therapist, it can be visualized in a dashboard after the session is completed. Further, the data is stored with a unique patient identifier so that the therapist can query the database to view the history of the patient's recovery over time. A complete video of the experiments performed for trajectory tracking and pick-and-place can be seen [28]. Fig. 12.

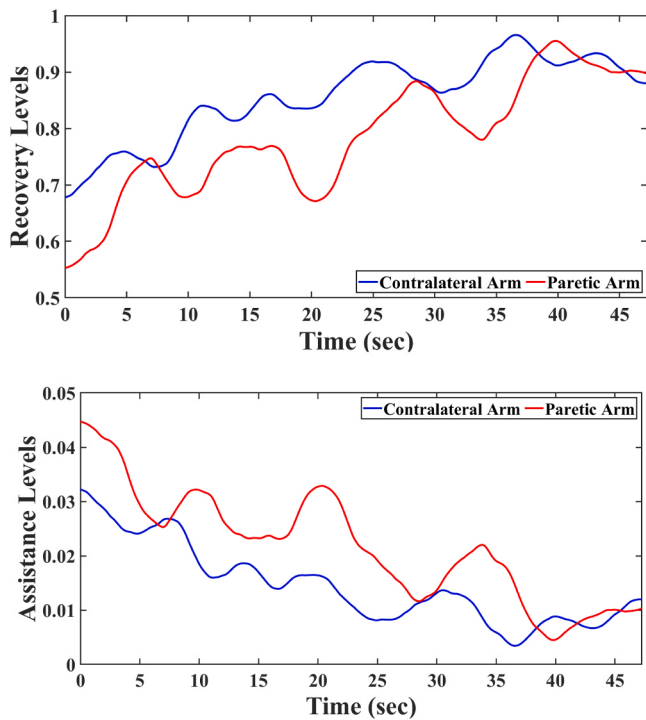


**Fig. 8.** Recovery and assistance levels.

### 5.5. Comparison with state-of-the-art

As detailed in [Section 1](#), RMT approaches undoubtedly have visible advantages over the traditional mirror therapy approaches. In addition, the proposed RMT solution also stands out in comparison to other RMT approaches. Though there are several robotic solutions proposed for rehabilitation in general, very few focus on the mirror therapy approach, although mirror therapy is an established standard in rehabilitation (see [Section 1](#) for details).

The state-of-the-art RMT approaches have been successful in creating a mirroring effect for both the patient's limbs but fall short in allowing

for the practice of ADL [\[13\]](#), which is a common practice in traditional mirror therapy. The framework proposed in this paper allows such ADL practice, encouraging the therapists to adopt this method as it fulfils their requirements. Even the trajectory tracking task (which is also a common task in traditional therapy) is facilitated in 3D while most earlier approaches are limited by 2D workspace of robots. Furthermore, while the state-of-the-art RMT approaches incorporated robots to exercise the patient's motor abilities in their limbs, clinical research also shows that for effective neuroplasticity, both motor and cognitive skill recovery must happen. For instance, in [\[13\]](#), the contralateral limb is provided with an impedance surface to track, but the paretic limb is only provided with a position controller. This means that the patient would not be able to independently make motions with their paretic limb. To facilitate the deliberate mirrored motion of the patient's paretic limb, some independent control (through the force controller described in [Section 4.5](#)) is provided to both the limbs. Though this might lead to poor initial tracking, the patient will be able to learn from their errors (through the assistive forces mentioned in [Section 2.3](#)), and more importantly also develop their cognitive abilities while attempting to deliberately keep their limbs in the mirrored positions. As already highlighted in [Section 4](#), the controllers developed in this work are robust enough to function within a wide range of controller gains. In the state-of-the-art RMT controllers [\[14,29,30\]](#), though the controllers are analytically proven to maintain stability and tracking, the therapist must go through the tedious task of choosing the gains for their specific patient. Furthermore, with the therapist's ability to choose  $\gamma$  and  $\sigma$ , the system can be patient specific.

In summary, each of the RMT approaches, i.e., from state-of-the-art and the proposed, attempt to accomplish the common goal in a significantly distinct manner. For this reason, only a qualitative comparison can be performed amongst these in the matter of the end features made available by each platform. A quantitative comparison would not be feasible given the diversity in implementation protocols. For instance, the position tracking errors, which are the primary metrics in the proposed work, cannot be compared with the position tracking error in other approaches since they operate in a 2D environment and within a different workspace. To present the qualitative standing of the present work, a feature-wise comparison is performed with traditional mirror therapy and state-of-the-art RMT and reported in [Table 1](#).

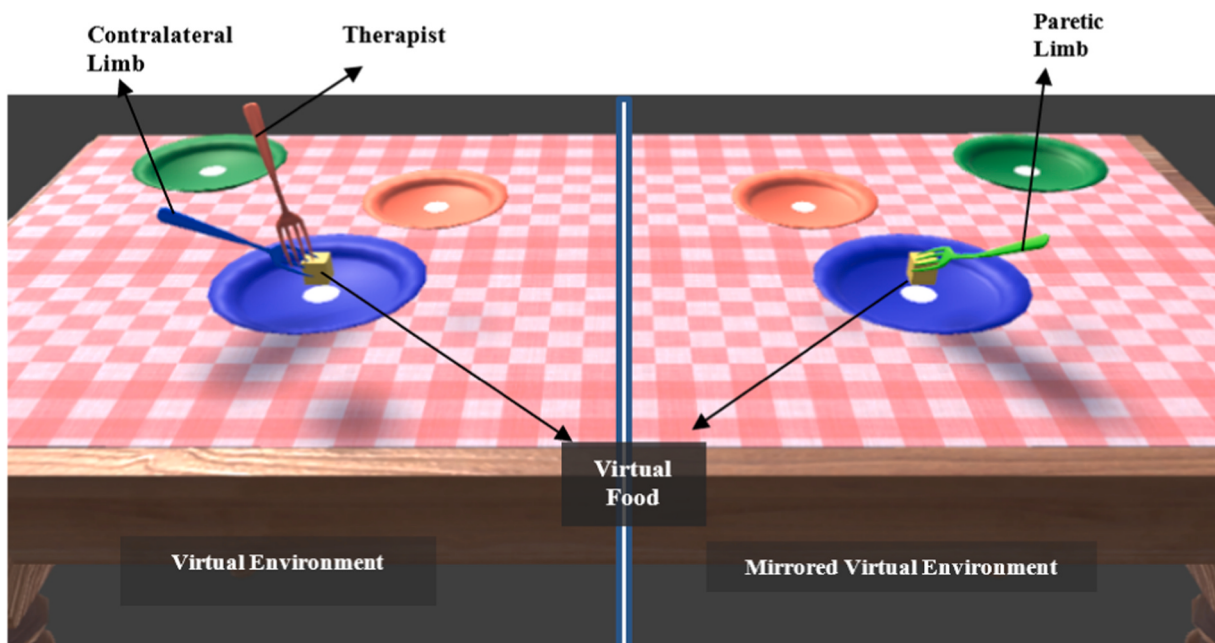


**Fig. 9.** Virtual environment for pick-and-place RMT.

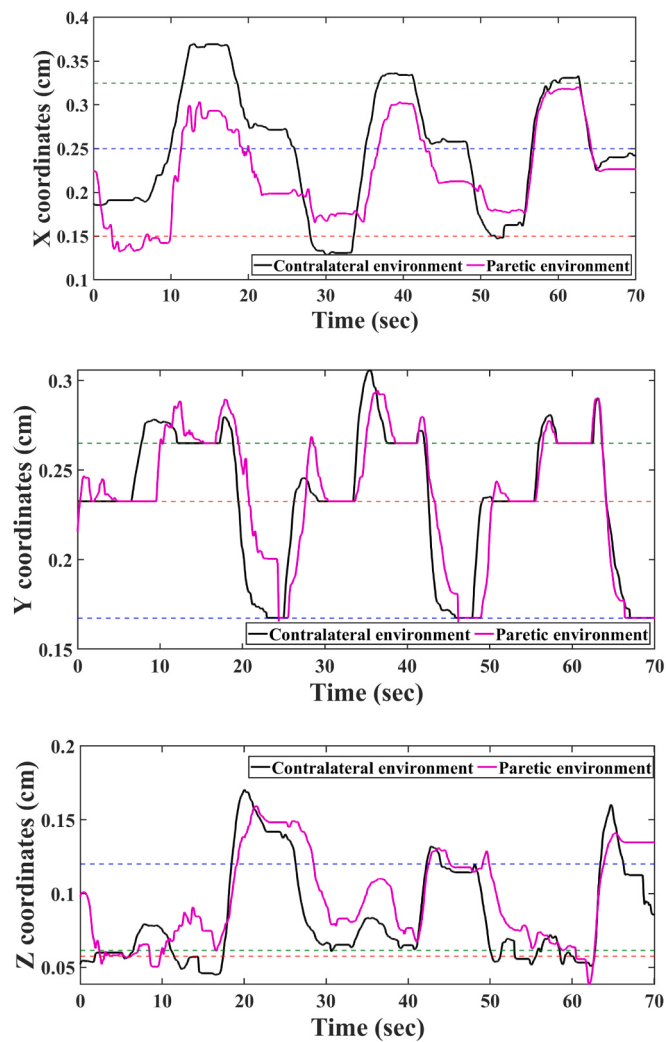


Fig. 10. Food trajectories in pick-and-place task.

### 5.6. Limitations

While the work presented here focuses on advancing RMT, it has some limitations. First, the experiments conducted here were done using healthy subjects. Future works will include studies to understand the benefits this RMT system may provide to real patients and therapists following protocols outlined in [17,31]. These studies will help to translate this work into a real clinical setting. Second, while the ADL implementation was enough to serve as a proof-of-concept, future works should include developing a more diverse library of such activities. Finally, technologies such as virtual reality can be incorporated into this system to enhance the realism and immersiveness of the activities, for example, by easing challenges related to depth perception in the ADL. In a similar way, the hardware used here was taken as off the shelf to allow for easy implementation of the system. To increase the effectiveness of the therapy, custom designed robotic devices may prove to be beneficial. Both virtual reality and custom hardware will be explored in future works.

### 6. Conclusions

To facilitate rehabilitation of patients with neurological disorders, a robotic mirror therapy framework is developed which can monitor and enhance the patient's motor, vision, and cognitive abilities, thus potentially encouraging neuroplasticity in them. The developed framework features dynamic monitoring of the recovery level in each of the

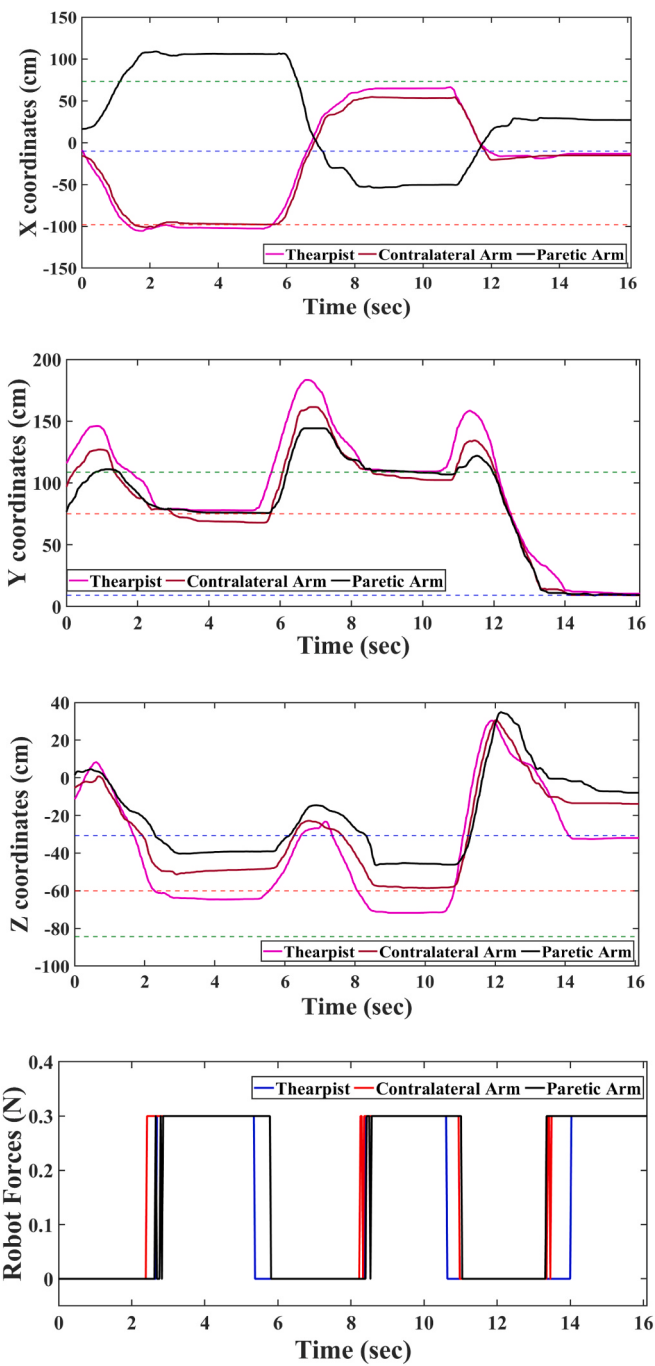


Fig. 11. Robot positions and forces when pressing against the plates.



Fig. 12. Visualization of the session results.

**Table 1**

Comparison of proposed RMT with traditional and state-of-the-art approaches.

	Traditional Mirror Therapy	State-of-the-art RMT[13]	Proposed RMT
Objective performance metrics	NO	YES	YES
Therapist to Patient Ratio	LOW	HIGH	HIGH
3D Tasks	YES	NO	YES
Incorporation of ADL	YES	NO	YES
Independent monitoring of motor and cognitive recovery	YES	NO	YES
No need for gain tuning	Not applicable	NO	YES
Degree of force-feedback	Full	Not applicable	Full
Patient's ability for independent learning	YES	NO	YES

patient's limbs, and correspondingly supplies assistance to carry out the task desired by the therapist. Controller design is also carried out using the nonlinear model of the robots, and passivity analysis is carried out to prove the accurate tracking and stability of the system. Experiments are then conducted with some common tasks involved in traditional therapy with healthy subjects. Results shown for trajectory tracking and pick-and-place tasks demonstrate the efficacy of the proposed framework and controllers.

#### CRediT authorship contribution statement

Harris Nisar – Conceptualization, Methodology, Software, Srikanth Annamraju – Conceptualization, Methodology, Project administration, Shankar Deka – Writing - review & editing, Anne Horowitz – Data curation, Conceptualization, Funding acquisition, Dusan Stipanovic – Funding acquisition, Supervision.

#### Declaration of Competing Interest

All the authors confirm that there is no conflict of interest.

#### Acknowledgments

The authors would like to thank the Jump ARCHES program, which is a collaborative effort between the Health Care Engineering Systems Center, University of Illinois Urbana Champaign, and the , for funding this research, under the grants P-291 and P-386.

#### Appendix A. Supporting information

Supplementary data associated with this article can be found in the online version at [doi:10.1016/j.csbj.2024.01.017](https://doi.org/10.1016/j.csbj.2024.01.017).

#### References

- [1] Feigin VL, et al. World stroke organization (WSO): global stroke fact sheet 2022. *Int J Stroke* 2022;17(1):18–29. <https://doi.org/10.1177/17474930211065917>.
- [2] Dimyan MA, Cohen LG. Neuroplasticity in the context of motor rehabilitation after stroke. *Nat Rev Neurol* 2011;7(2):76–85. <https://doi.org/10.1038/nrneurol.2010.200>.
- [3] Tsao CW, et al. Heart disease and stroke statistics—2023 update: a report from the American heart association. *Circulation* 2023;147(8). <https://doi.org/10.1161/CIR.0000000000001123>.
- [4] Ingwersen T, et al. Long-term recovery of upper limb motor function and self-reported health: results from a multicenter observational study 1 year after discharge from rehabilitation. *Neurol Res Pract* 2021;3(1):66. <https://doi.org/10.1186/s42466-021-00164-7>.
- [5] Kwakkel G, Kollen BJ, Van Der Grond J, Prevo AJH. Probability of regaining dexterity in the flaccid upper limb: impact of severity of paresis and time since onset in acute stroke. *Stroke* 2003;34(9):2181–6. <https://doi.org/10.1161/01.STR.0000081712.16305.CD>.
- [6] Mercier L, Audet T, Hebert R, Rochette A, Dubois M-F. Impact of motor, cognitive, and perceptual disorders on ability to perform activities of daily living after stroke. *Stroke* 2001;32(11):2602–8. <https://doi.org/10.1161/hs1101.098154>.
- [7] Altschuler EL, et al. Rehabilitation of hemiparesis after stroke with a mirror. *Lancet* 1999;353(9169):2035–6. [https://doi.org/10.1016/S0140-6736\(99\)00920-4](https://doi.org/10.1016/S0140-6736(99)00920-4).
- [8] Pérez-Cruzado D, Merchán-Baeza JA, González-Sánchez M, Cuesta-Vargas AI. Systematic review of mirror therapy compared with conventional rehabilitation in upper extremity function in stroke survivors. *Aust Occup Ther J* 2017;64(2):91–112. <https://doi.org/10.1111/1440-1630.12342>.
- [9] Louie DR, Lim SB, Eng JJ. The efficacy of lower extremity mirror therapy for improving balance, gait, and motor function poststroke: a systematic review and meta-analysis. *J Stroke Cerebrovasc Dis* 2019;28(1):107–20. <https://doi.org/10.1016/j.jstrokecerebrovasdis.2018.09.017>.
- [10] Kelso JAS, Southard DL, Goodman D. On the nature of human interlimb coordination. *Science* 1979;203(4384):1029–31. <https://doi.org/10.1126/science.424729>.
- [11] Cauraugh JH, Kang N. Bimanual movements and chronic stroke rehabilitation: looking back and looking forward. *Appl Sci* 2021;11(22):10858. <https://doi.org/10.3390/app112210858>.
- [12] Cramer SC, et al. Harnessing neuroplasticity for clinical applications. *Brain* 2011;134(6):1591–609. <https://doi.org/10.1093/brain/awr039>.
- [13] Shahbazi M, Atashzad SF, Tavakoli M, Patel RV. Robotics-assisted mirror rehabilitation therapy: a therapist-in-the-loop assist-as-needed architecture. *IEEE/ASME Trans Mechatron* 2016;21(4):1954–65. <https://doi.org/10.1109/TMECH.2016.2551725>.
- [14] Xu J, et al. A multi-channel reinforcement learning framework for robotic mirror therapy. *IEEE Robot Autom Lett* 2020;5(4):5385–92. <https://doi.org/10.1109/LRA.2020.3007408>.
- [15] Xu J, Xu L, Ji A, Cao K. Learning robotic motion with mirror therapy framework for hemiparesis rehabilitation. *Inf Process Manag* 2023;60(2):103244. <https://doi.org/10.1016/j.ipm.2022.103244>.
- [16] Ruggiu M, Rea P. Development of a mechatronic system for the mirror therapy. *Actuators* 2022;11(1):14. <https://doi.org/10.3390/act1101014>.
- [17] Beom J, et al. Robotic mirror therapy system for functional recovery of hemiplegic arms. *JoVE* 2016;(114):54521. <https://doi.org/10.3791/54521>.
- [18] Rensink M, Schuurmans M, Lindeman E, Hafsteinsdóttir T. Task-oriented training in rehabilitation after stroke: systematic review. *J Adv Nurs* 2009;65(4):737–54. <https://doi.org/10.1111/j.1365-2648.2008.04925.x>.
- [19] Thant AA, et al. Effects of task-oriented training on upper extremity functional performance in patients with sub-acute stroke: a randomized controlled trial. *J Phys Ther Sci* 2019;31(1):82–7. <https://doi.org/10.1589/jpts.31.82>.
- [20] Rapoport J, Endzelytė E, Jasevičienė I, Savickas R. Stroke patients motivation influence on the effectiveness of occupational therapy. *Rehabil Res Pract* 2018; 2018:1–7. <https://doi.org/10.1155/2018/9367942>.
- [21] Yoshida T, Otaka Y, Osu R, Kumagai M, Kitamura S, Yaeda J. Motivation for rehabilitation in patients with subacute stroke: a qualitative study. *Front Rehabilit Sci* 2021;2:664758. <https://doi.org/10.3389/fresc.2021.664758>.
- [22] Anderson RJ, Spóng MW. Bilateral control of teleoperators with time delay. *IEEE Trans Autom Contr* 1989;34(5):494–501. <https://doi.org/10.1109/9.24201>.
- [23] H.K. Khalil, Nonlinear Systems. in Pearson Education, Prentice Hall, 2002. [Online]. Available: [https://books.google.com/books?id=t\\_d1QgAACAAJ](https://books.google.com/books?id=t_d1QgAACAAJ).
- [24] J.J. Craig, Introduction to robotics: mechanics and control, 3rd ed. Upper Saddle River, N.J: Pearson/Prentice Hall, 2005.
- [25] E. S J-J, Li W. Applied Non-Linear Control. Prentice Hall.; 1991.
- [26] Raibert MH, Craig JJ. Hybrid position/force control of manipulators. *J Dyn Syst, Meas, Control* 1981;103(2):126–33. <https://doi.org/10.1115/1.3139652>.
- [27] Gladstone DJ, Daniels CJ, Black SE. The Fugl-Meyer assessment of motor recovery after stroke: a critical review of its measurement properties. *Neurorehabil Neural Repair* 2002;16(3):232–40. <https://doi.org/10.1177/154596802401105171>.
- [28] Robotic mirror therapy demo video. [Online Video]. Available: [https://www.youtube.com/watch?v=HVajXPREwpk&ab\\_channel=HarrisNisar](https://www.youtube.com/watch?v=HVajXPREwpk&ab_channel=HarrisNisar)
- [29] Marchal-Crespo L, Reinkensmeyer DJ. Review of control strategies for robotic movement training after neurologic injury. *J Neuroeng Rehabil* 2009;6(1):20. <https://doi.org/10.1186/1743-0003-6-20>.
- [30] Sharifi M, Behzadipour S, Salarieh H, Tavakoli M. Cooperative modalities in robotic tele-rehabilitation using nonlinear bilateral impedance control. *Control Eng Pract* 2017;67:52–63. <https://doi.org/10.1016/j.conengprac.2017.07.002>.
- [31] Chen Y-W, Li K-Y, Lin C-H, Hung P-H, Lai H-T, Wu C-Y. The effect of sequential combination of mirror therapy and robot-assisted therapy on motor function, daily function, and self-efficacy after stroke. *Sci Rep* 2023;13(1):16841. <https://doi.org/10.1038/s41598-023-43981-3>.